RESEARCH PAPER

Preparation and Characterization of New Nano composite Spinel Oxide and Study of Its Chemical Activity in Removal of Indigo Carmine Dye

Hussein Turkey *, Angham G. Hadi

Department of Chemistry, College of Science, Babylon University, Babil 51002, Iraq

ARTICLE INFO

Article History: Received 08 March 20223 Accepted 22 May 2023 Published 01 October 2025

Keywords:

Copper oxide Manganese oxide Indigo carmine dye Spinel oxide Co-precipitation

ABSTRACT

Spinel oxide exhibits numerous advantageous properties, leading to enhanced performance in various applications such as catalysis, sensing, batteries, dye degradation and drug storage. A significant area of current research revolves around its potential to eliminate organic pollutants from wastewater, addressing environmental concerns. In a particular study, we prepared manganese-copper oxide catalyst alone and supported by magnesium oxide by co- perception method via calcination at different temperatures of 500 and 600°C. The resulting powder of prepared precursors was characterized by X-ray diffraction (XRD), Fourier transform infrared spectroscopy (FTIR), Energy dispersive x-ray technique (EDS) and scanning electron microscopy (SEM). The catalytic activity of the prepared catalyst was investigated by removing (97.3%) of indigo carmine dye from the effluents of textile wastewater by adsorption and photocatalytic degradation; the reaction was followed by a UV/Vis spectrophotometer at λ max =610 nm. The optimum conditions of temperature and contact time and weight were studied to find out which catalysts gave the highest dye removal efficiency.

How to cite this article

Turkey H., Hadi A. Preparation and Characterization of New Nano composite Spinel Oxide and Study of Its Chemical Activity in Removal of Indigo Carmine Dye. J Nanostruct, 2025; 15(4):2260-2270. DOI: 10.22052/JNS.2025.04.065

INTRODUCTION

Water composition varies depending on its source and location, encompassing a range of organic and inorganic substances. Disruption of these concentrations leads to pollution. To ensure water quality, national and international standards dictate permissible concentration levels [1]. Numerous industries, such as pharmaceuticals, leather, textiles, paper and oil refineries, generate wastewater containing diverse organic and inorganic substances. The specific materials present contribute to the variation in organic matter. Some materials are

hazardous and resistant to decomposition, while others are less harmful and readily biodegradable. Pollutants in dye industry wastewater and domestic water encompass a wide range of substances, including inorganic compounds, heavy metal ions and organic pollutants. Among the effective techniques employed for purification and separation processes, adsorption is widely recognized. The extensive utilization of adsorption in various purification procedures has attracted the attention of numerous scholars due to its remarkable contributions. Several methods are available for removing dyes from wastewater,

^{*} Corresponding Author Email: analhusainy@gmail.com

including chemical oxidation, adsorption, chemical reduction, photo-degradation, electrochemical oxidation, coagulation-flocculation, membrane separation, Fenton oxidation and biological approaches. Each of these methods has its own advantages and disadvantages [2]. In fact, adsorption processes have become indispensable in modern industries, presenting a challenge for any sector to operate without encountering them [3]. Adsorption, also known as amaze, refers to the process by which substance molecules are gathered onto the surface of a solid material. When multiple layers of molecules are present during adsorption, it is referred to as multimolecular adsorption [4, 5]. The regular configuration of a spinel comprises from the chemical formula AB2O4. In this configuration, A typically represents a divalent cation occupying the tetrahedral sites, while B usually represents a trivalent cation occupying the octahedral sites within the cubic structure of the spinel. Another spinel structure, known as the "inverse" structure, can be expressed as $B(AB)O_4$. In this structure, B represents a trivalent metal cation, with half of these cations occupying the tetrahedral sites and the other half occupying the octahedral sites. Meanwhile, A, a divalent metal cation, occupies an octahedral site within the spinel structure [6, 7]. Photocatalysts in wastewater treatment often utilize transition metal oxides, which are compounds formed when oxygen atoms combine with transition metals [8]. These materials have proven to be effective in various applications. Among the different metal oxides found in minerals, Manganese oxide (MnO) is particularly abundant in soil, sediment and aquifers. However, the efficacy of natural MnO minerals as absorbents for specific dyes can vary due to impurities and differences in their composition and structure. To overcome these variations, several research teams have turned to synthesized MnO minerals with precise composition and structure. By using these tailored materials, they aim to better assess their effectiveness as sorbents for dye removal from solutions and as catalysts for dye degradation. This approach allows for a more controlled evaluation of the materials' performance in these applications [9, 10]. The pursuit of economical catalysts has been intensified due to the scarcity and expensive nature of precious metals. Overall, the performance of copper manganese blended oxides is attributed to the creation of a CuMnO hybrid that lacks a definite structure. This hybrid results from the interaction of copper and manganese oxides [11, 12]. The relative proportion of copper (Cu) and manganese (Mn) is a critical factor that profoundly influences the phase composition of catalysts produced. Scientific reports indicate that the most efficient catalytic performance occurs when the Cu/Mn ratio is maintained at 1:1 [13, 14]. Moreover, the characteristics and properties of the catalyst supports also have a discernible impact on their catalytic capabilities. The interaction between the metal and support is particularly noteworthy, as it contributes to the observed outcomes. Consequently, there has been a significant focus on investigating the relationship between the active ingredient and the support, as it plays a vital role in enhancing our understanding of the catalytic processes exhibited by these catalysts. Among the various CuMn catalysts with support, particular attention has been given to Cu-Mn-O/MgO. This specific catalyst system has emerged as a focal point of interest. In comparison to CuO/MnO catalysts, CuO-MnO/ MgO exhibits superior effectiveness in eliminating hazardous dyes. This can be attributed to the MnO compounds extending their coverage onto the CuO, resulting in enhanced catalytic performance and efficiency. To create the CuO-MnO/MgO catalyst, copper oxide and manganese oxide were combined in a ratio of 20% copper and 40% manganese. This mixture was then embedded onto magnesium oxide at a concentration of 40%. The catalyst, along with its supported counterpart, underwent roasting at elevated temperatures ranging from 500 to 600 °C [15]. Indigo (Fig. 1) is a dye of significant historical and practical importance, commonly utilized for dyeing clothes such as blue jeans and denim. However, due to its low solubility in water (<2 mg l-1), indigo must be transformed into more soluble products before industrial application. One common transformation involves reacting indigo with sulfuric acid, resulting in indigo carmine. Indigo carmine is a widely used dye for coloring food, serving as an indicator in analytical chemistry and functioning as a microscopic stain in biology [16, 17]. The aim of this project is to produce a spinelsupported catalyst using the co-precipitation method, specifically Cu-Mn-O/MgO. The catalyst will be analyzed using various spectroscopic techniques to evaluate its properties. Additionally, the project aims to investigate the effectiveness

of this catalyst in removing indigo carmine dye through either adsorption or photo-degradation processes.

MATERIALS AND METHODS

Preparation spinel oxide (CuMnO)

The catalyst precursors were produced using the co-precipitation method. Copper nitrate Cu(NO₂)₂.3H₂O weighing 6.06 gm and manganese acetate Mn(CH₃COO)₃•4H₃O weighing 6.9 gm were dissolved in separate aqueous solutions. The solutions were then mixed to achieve a molar ratio of 1:1 for Cu and Mn. The resulting solution was heated between 60-70°C. A 0.5 M aqueous solution of sodium carbonate (Na₂CO₂) was slowly added drop by drop to the solution while stirring continuously at 140 rpm. The temperature was maintained at 80°C until the pH reached a range between 9.0 and 9.3, which typically took about 10 to 15 minutes. The resulting precipitate was aged in this medium for varying durations from 0 to 240 minutes. Afterward, the precipitate was filtered and washed multiple times with hot and cold distilled water until the sodium content, as measured by atomic absorption, was below approximately 140 ppm. The precipitate was then dried at 100°C for 16 hours, resulting in a material referred to as the catalyst precursor. The catalyst precursor was further processed through calcination at 500°C for 4 hours and 600°C for 4 hours to obtain the final catalyst product [18].

Preparation spinel oxide with supported (Cu-Mn-O/MgO)

The catalyst was created using the coprecipitation method, where the same conditions were utilized with the support material, but a difference in proportions was made. A fitting amount of magnesium nitrate support poultice, weighing 25.44 gm, was taken into account. Magnesium oxide 40 % was mixed with copper oxide and manganese oxide at a proportion of 20% copper and 40% manganese then incorporated into the compound at a concentration of 100%. The fulfillment of the task coincides with the requirements stated in the preceding step.

Characterization

Powder X-ray diffraction (PXRD)

Samples of synthesized spinel catalyst were studied by PXRD at different temperatures, using a Shimadzu XRD-6000 with $CuK\alpha$ radiation. Phase identification was done by comparing the sample X-ray pattern with JCPD standards. Crystallite size was calculated using the Debye Scherer equation: $D = K\lambda/\cos\theta$, with K = 0.89 and diffraction line broadening measured in radians at half maximum intensity (nm) [19].

FT-IR

The supported (CuMn₂O₄/MgO) and without supported (CuMn₂O₄) catalyst samples were examined using infrared spectroscopy (IRAFFINTY-1, Germany) within the range of 4000-400 cm⁻¹, with KBr powder being utilized [20].

SFM

The composite and individual compounds were imaged using HRSEM. XPS was used to evaluate the surface electron state and composition catalyst of supported and unsupported (CuMnOx) and (CuMn₂O₄/MgO) composites [21].

Energy dispersive X-ray (EDX)

EDX was used to analyze the chemical composition of spinel supported and unsupported catalysts. A specialized model (INCAX-act) was used, with a resolution of 5.9 kV, to obtain localized

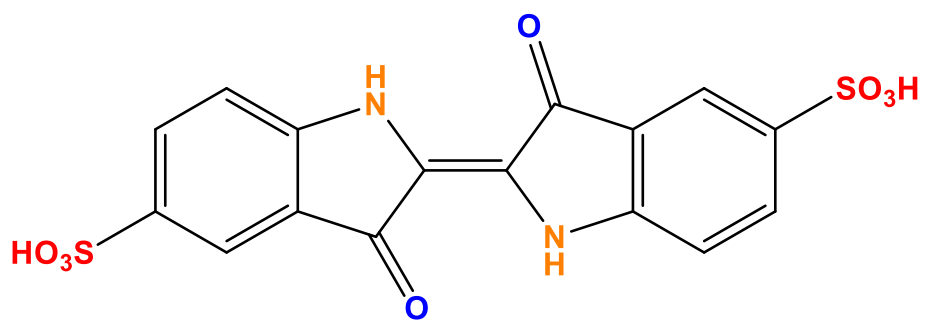


Fig. 1. The chemical composition of indigo carmine dye.

data on the elements present.

Photocatalytic and adsorption

Supported and unsupported catalysts' activity compared using the adsorption and photocatalytic degradation of 50 ppm indigo carmine dye at 610 nm.

Practical application

The photoreaction cell is composed of a Pyrex glass container featuring a quartz window and is equipped with a Philips Holland lamp (250 W) for radiation. The entire apparatus has a volume of 30 mL and is of homemade construction. The catalysts were readied and divided into different amounts (0.025, 0.050, 0.075, 0.100 and 0.125grams), both with and without support. These were then introduced into a reaction cell containing 30 mL of indigo carmine dye with a concentration of 50 ppm. The reaction at 25 °C and the reaction were started through adsorption, lasting for only 15 minutes before withdrawing 3mL from the mixture. Next, expose the reaction mixture to ultraviolet radiation for 60 minutes and collect 3mL samples at 15-minute intervals until the end of the reaction time. After gathering the samples, they were cautiously centrifuged to avoid the creation of sizable particles with the excess liquid. The UV-visible double beam spectrophotometer (Shimadzu 6100 PC, Germany) was used to measure the absorbance of indigo carmine dye at 610 nm.

The removal efficiency of indigo carmine dye was determined:

Removal Efficiency (R.E) = $(A_a - A_b / A_a) \times 100\%$

A_o = initial absorbance at time zero. A_o = absorbance at time t.

RESULTS AND DISCUSSION

Fig. 2 displays the XRD patterns of the CuMn₂O₄ catalyst spinel phase at temperature 500 °C. All samples show similar diffraction peaks at 2θ = 30.3°, 36.9°, 43.4°, 57.6° and 63.2°, suggesting that the major phases are mixtures of copper manganese hybrid oxide (CuMnO_x, JCPDS No. 41-0182) and manganese oxide (Mn₂O₃, JCPDS No. 33-0900). The diffraction peak at $2\theta = 35.7^{\circ}$ indicates the presence of amounts of copper oxide (CuO, JCPDS No. 35-1472). At the catalyst, while at high temperature 600 °C begin the dispersion of oxide and can be noted this by presence of different peaks due to the crystallite structure for catalyst was increased with increased of calcination temperature and formation the spinel type complex oxide of CuMnO. The low resolution of the diffraction peaks indicates that the samples are poorly crystallized. These results are consistent with previous reports of amorphous prepared by co-precipitation [22-23].

Fig. 3 presents the XRD patterns of prepared spinel supported catalyst ($CuMn_2O_4/MgO$) indicated beginning the formation of desired phase at low temperature 500 $^{\circ}$ C, while at high temperature 600 $^{\circ}$ C begin the dispersion of oxide and can be noted this by presence of different peaks due to the crystallite structure for supported catalyst was increased with increased of calcination temperature [24].

FTIR analysis at 500-600°C identified metal-oxygen and metal-metal bonds in CuMn₂O₄ spinel

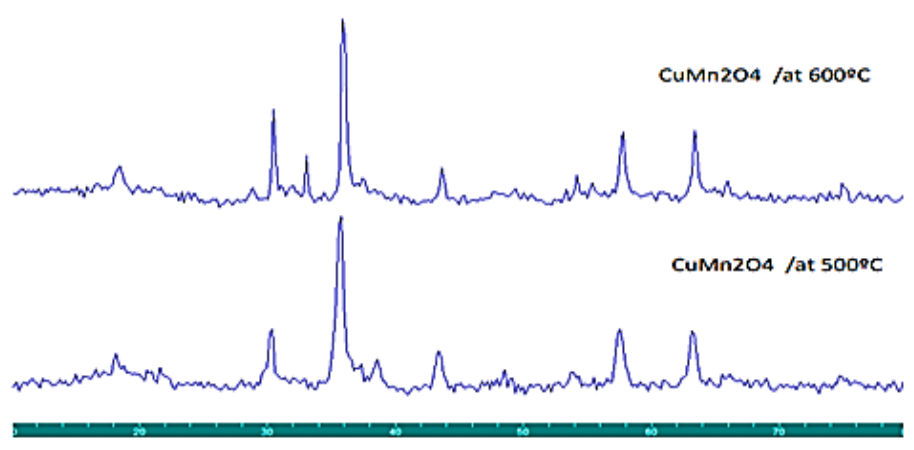


Fig. 2. Show XRD pattern of spinel oxides $CuMn_2O_4$.

catalyst (Fig. 4), observed at 2000-400 cm $^{-1}$ Low frequency. Vibrations of M-O bond <1000 cm $^{-1}$ shown in Fig. 4.The peaks at 599.86 and 451.34 cm $^{-1}$ are evidence of CuMn $_2$ O $_4$ formation, representing Cu–O and Mn-O stretching modes. The peak at 651.94 cm $^{-1}$ is Cu–Mn stretching vibration and the 1000-1400 cm $^{-1}$ band is due to -OH vibration. These vibrations are unique to metal oxides in spinel [25].

FTIR at 500-600°C identified metal-oxygen and metal-metal bonds. Supported catalyst oxides

 $(\text{CuMn}_2\text{O}_4/\text{MgO})$ showed vibrations in the region 600-400 cm⁻¹, attributed to M-O vibrations (where M = Cu, Mn, Mg). The peak at 500 cm⁻¹ corresponds to an Mg-O vibrational band attributed to the supporter. At 490 cm⁻¹, Cu-O stretching vibration mode was observed along with corresponding peaks for Cu-O bond at 600 and 430 cm⁻¹. Peaks at 410, 600 cm⁻¹ were attributed to O-Mn-O bond due to resonances between metal center and oxygen atoms (Fig. 5). Weak absorption bands at 1500 cm⁻¹ show no absorbed moisture [26].

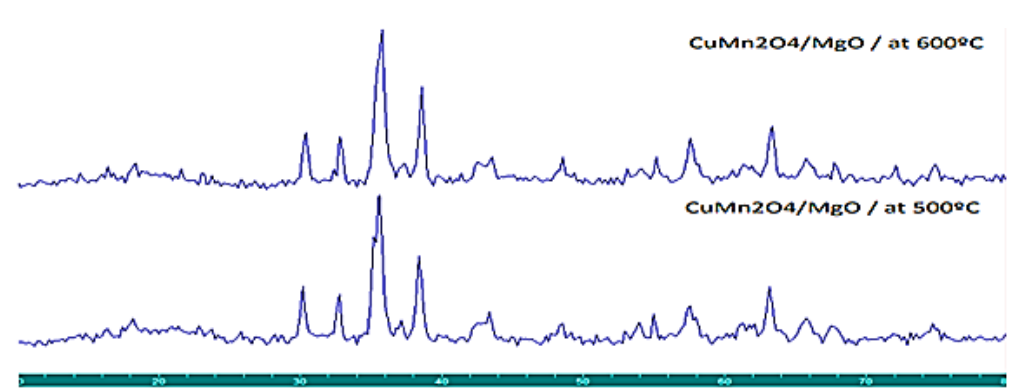
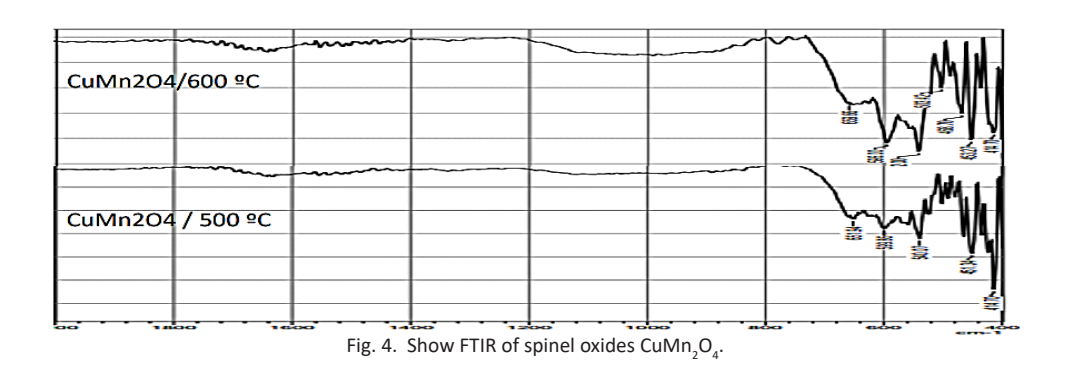


Fig. 3. Show XRD pattern of supported spinel oxides CuMn₂O₄/MgO.



CulMn2O4/MgO / 600 °C

Fig. 5. Show FTIR of supported spinel oxides CuMn₂O₄/MgO.

 ${\rm CuMn_2O_4}$ SEM image shows spherical granular particles size. Showed ${\rm CuMn_2O_4}$ nanoparticle morphology prepared degree at 500°C in particles size 45 nm almost and 600°C 75 nm almost (Fig. 6a-c). Process temperature impacts ${\rm CuMn_2O_4}$ nanoparticle uniformity (Fig 6b-d, SEM images at 5 μ m scale). SEM images show that 500°C yields fine ${\rm CuMn_2O_4}$ nanoparticles, while 600°C causes clumping. The SEM image shows even distribution of rice-shaped nanoparticles with different sizes in the nano scale region (Fig. 6). The results suggest that the uniform distribution of nanoparticles enhances the surface-to-volume ratio, increasing the catalyst properties and acts as an adsorbent for dye molecules [27].

SEM image shows dimensions and surface features of the produced samples prepared degree at 500° C and 600° C, with a scale of 500 nm and 5 μ m. The use of $\text{CuMn}_2\text{O}_4/\text{MgO}$ showed that the surface was uneven and consisted of concave spherical shapes, implying the influence of the magnesium oxide support material's structure (Fig. 7) the structure of something can provide opportunities for the development of empty spaces that can serve as a medium for adsorbing

dye molecules. The dimensions of the flake-shaped structure have been determined [28,29].

The present study illustrates the elemental compositional analysis of a nanomaterial catalyst supported by CuMn₂O₄/MgO, as depicted in (Fig. 8). The Mn and Cu, as well as their respective ratios with Mg, were ascertained via Energy Dispersive X-ray (EDX) analysis, revealing congruence with CuMn₂O₄/MgO. The aforementioned information substantiates the existence of copper, manganese, and magnesium, wherein their weights account for 8.66%, 46.18% and 46.16% of the composition, and their atomic percentages correspond to 4.81%, 29.65% and 65.54%, respectively. The observed outcome bears a significant resemblance to the initial stoichiometric value [30].

Study the optimal condition to removal dye by monitoring UV-Vis spectrophotometer
The effect of calcination temperature

The analysis of the spectra for samples subjected to varying calcination temperatures was examined to determine the impact on the properties of the prepared catalysts. Changes were noted in the absorption edges when the temperature for

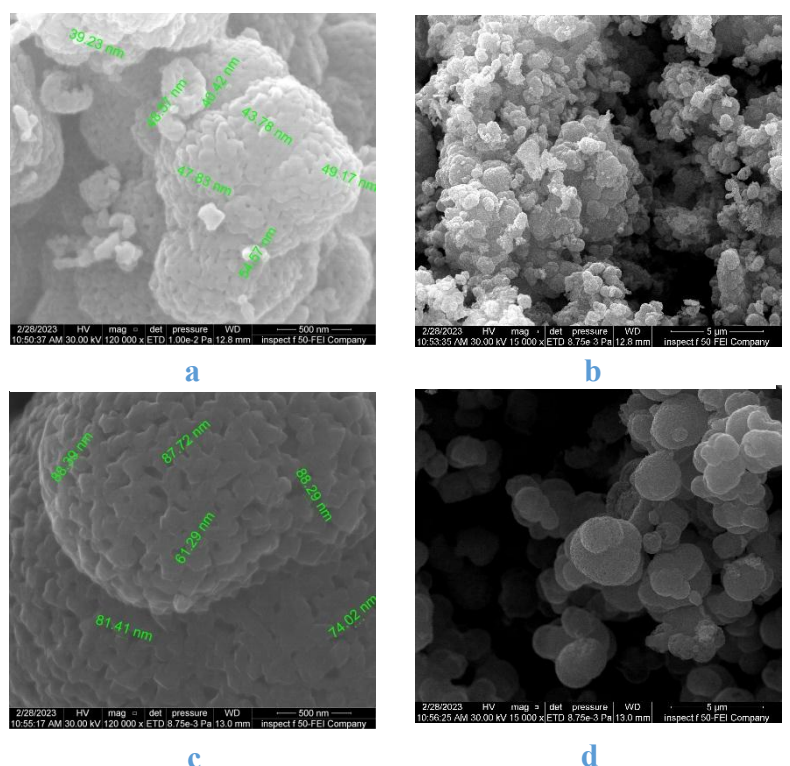


Fig. 6. Show SEM of spinel oxides CuMn₂O₄.

calcination was modified. According to the Fig. 8, the most effective temperature for removal indigo carmine dye (50 ppm) from the industrial textile wastewater in using a catalyst is 500°C, this may be due to the increasing of active sites and best pore size distribution in surface and also present the copper and manganese in two different oxidation states which increases the efficiency of oxidation

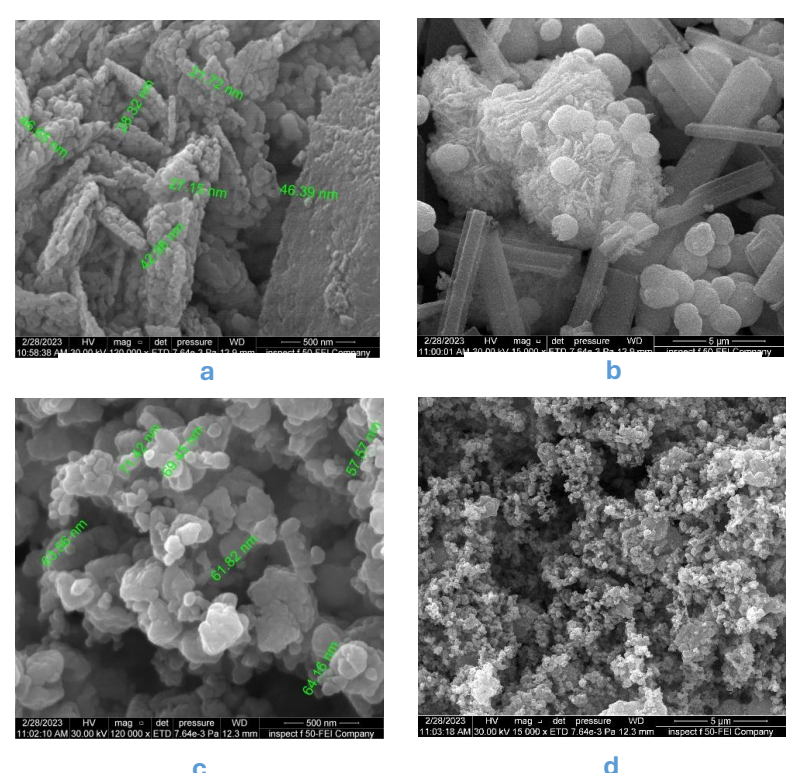


Fig. 7. Show SEM of supported spinel oxides CuMn₂O₄/MgO.

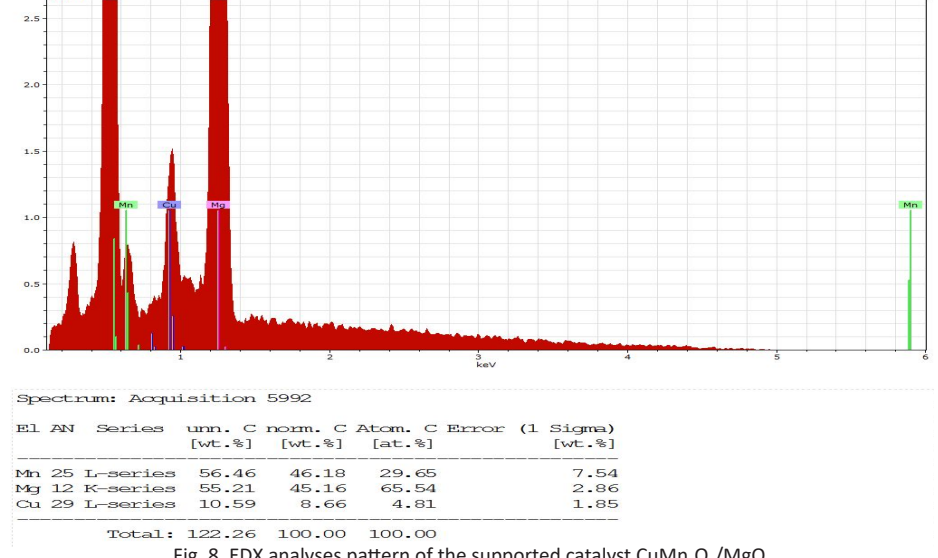


Fig. 8. EDX analyses pattern of the supported catalyst CuMn₂O₄/MgO.

and reduction process but if the temperature is raised to 600°C, the catalyst's surface will become stuck together and become inactive (Fig. 9) [31,32].

Effect of contact time on % removal dye

Study on effect of contact time on dye removal: Removal % increased to 99% with increasing time from 15 to 60 min, but reached saturation and equilibrium.

The Figs. 10 and 11 suggest that the most effective duration of time for removing indigo carmine dye is 30 minutes. Moreover, the utilization of magnesium oxide as a supporting substance during photocatalytic (Fig. 11b) treatment leads

to a surge in the level of dye elimination owing to its ability to amplify the catalytic surface area and stimulate the functional sites.

Effect of catalysts Dosage on % removal dye

The adsorbent amount for indigo carmine dye adsorption in aqueous solutions is a crucial parameter for designing a photocatalytic or adsorption system. Fig. 12 shows Catalyst dosage varied from 0.025-0.125gm and different times, ranging from 15-60 min, were tested while keeping other conditions constant. Dye at 50 ppm removed at 500 °C using equation. Fig. 12 show that removal efficiency rose from 15.8% to 97.3% at a dosage increase from 0.025 to 0.050gm.

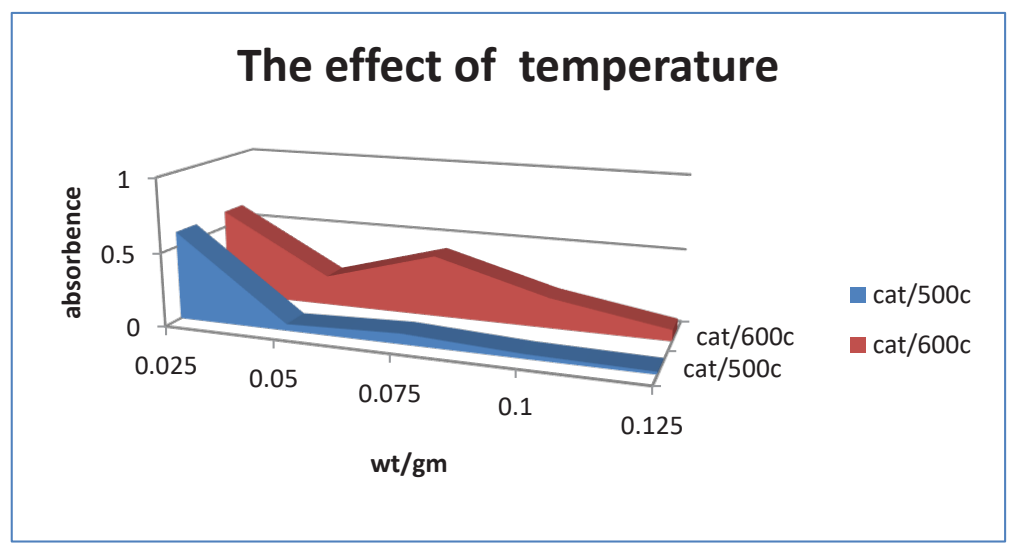


Fig. 9. The effect of calcination temperature on the properties of CuMn₂O₄/MgO.

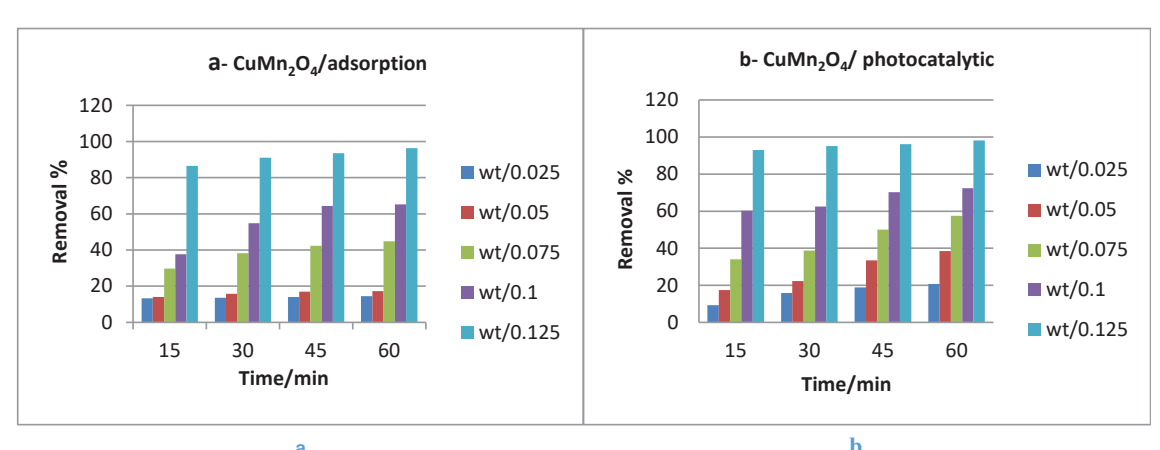


Fig. 10. The effect of adsorption and photocatalytic on removal dye in presences of CuMn₂O₄ alone.

Increasing the dosage of from 0.050 to 0.125gm did not significantly improve removal efficiency. Higher dosage increases active site, improving removal efficiency. Too many active sites caused saturation of adsorption. Optimal dosage for removing indigo carmine dye (0.05gm) at time 30min [33].

Effect of Photocatalytic and adsorption on % removal dye

Generally, if photons of appropriate energy, that is, the surface of (CuMn₂O₄/MgO) captures the dye solution when the energy level is above the band gap. Once light is absorbed, the electrons

in the valence band become excited and move to the conduction band, creating voids in the valence band. By combining with oxygen, electrons have the capability to create superoxide radicals which in turn can trigger the photo degradation of organic dye and pollutants, proving that using photocatalytic methods is more effective in removal dyes and the role of the supporting material is clear as demonstrated in Fig. 13 with a rate of 97.3%. During the photocatalytic reaction, the performance of (CuMn₂O₄/MgO) samples in removal indigo carmine dye was well by the calcination temperature, as revealed through experimentation with varying temperatures. The

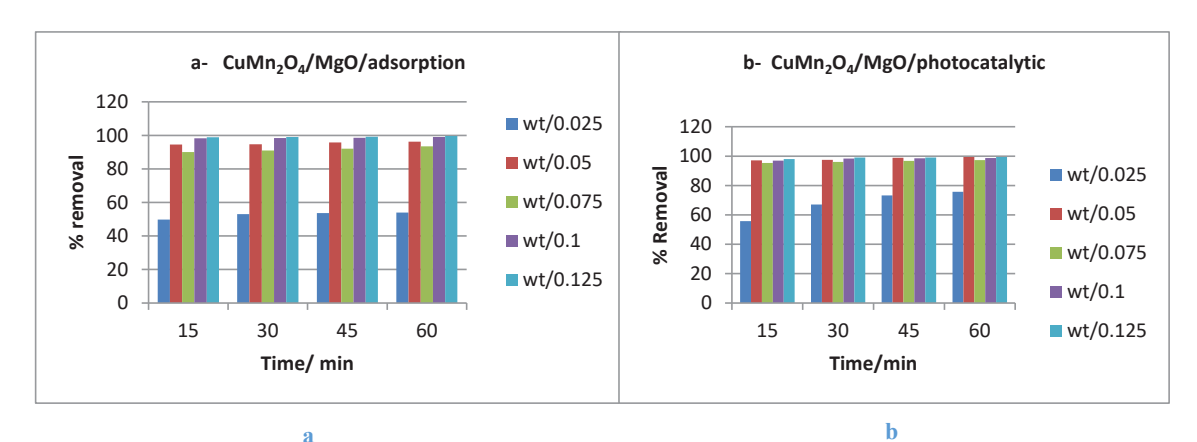


Fig. 11. The effect of adsorption and photocatalytic on removal dye in presences of CuMn₂O₄/MgO.

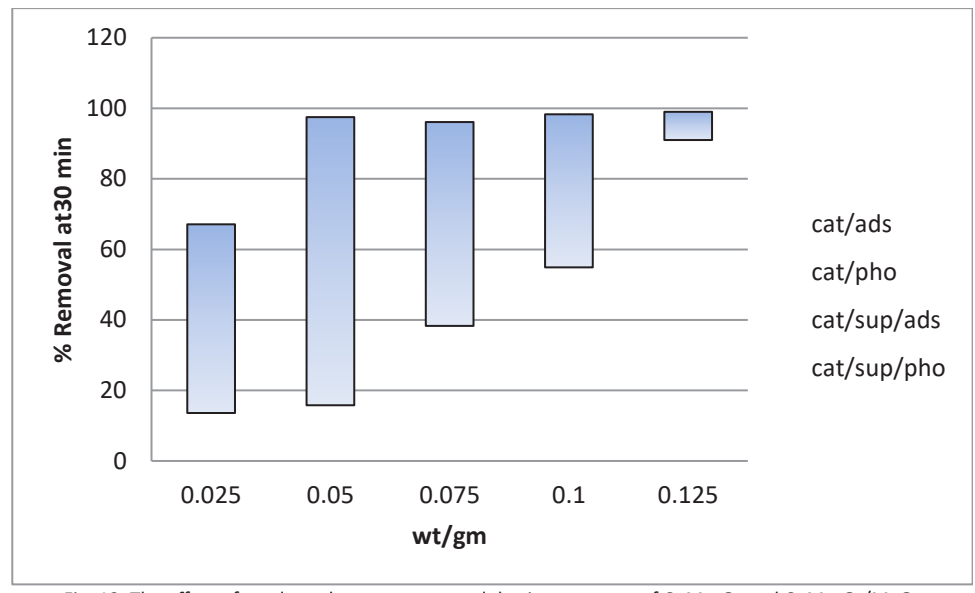


Fig. 12. The effect of catalysts dosage on removal dye in presences of ${\rm CuMn_2O_4}$ and ${\rm CuMn_2O_4}/{\rm MgO}$.

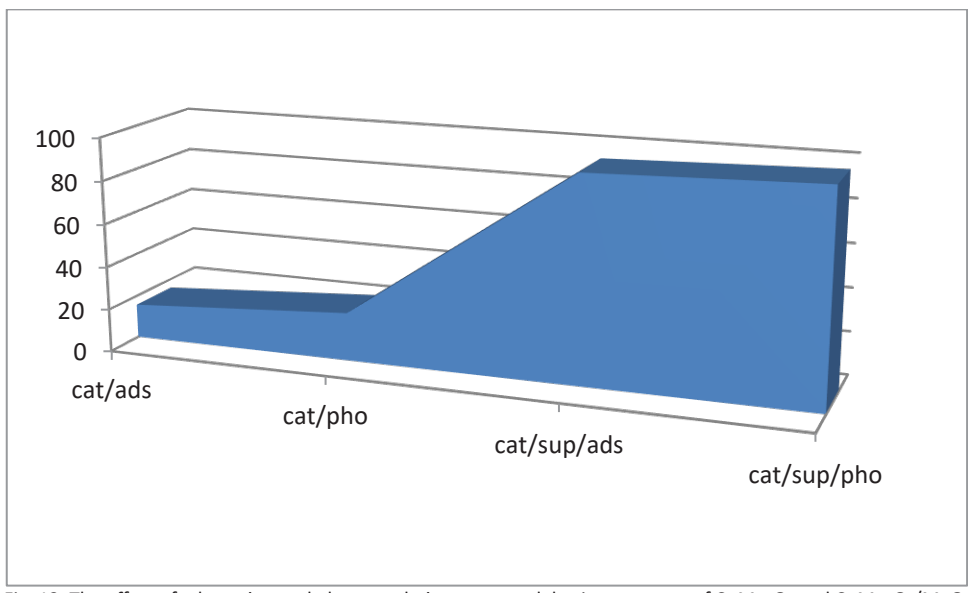


Fig. 13. The effect of adsorption and photocatalytic on removal dye in presences of CuMn,O, and CuMn,O,/MgO.

photoactivity of ($CuMn_2O_4/MgO$) at a weight of 0.050gm and a 30-minute contact time for the indigo carmine dye was found to increase at calcination temperatures up to 500°C. (Fig. 13) However, exceeding this temperature may lead to a decline in its activity [34].

CONCLUSION

The outcome shows that the formation of the $\text{CuMn}_2\text{O}_4/\text{MgO}$ supported spinel catalyst commenced at a temperature of 500 °C. The catalysts' particle size was determined using SED, with recorded sizes of 21.72, 28.23 and 46.65 nm. The block used in preparation matched the calculated cluster using EDX. The findings show that the spinel phase crystalline has superior efficiency in removing (97.3%) of indigo carmine dye at 500 °C. The optimal catalyst weight for photocatalytic reaction was determined to be 0.05 gm. at contact time 30min.

CONFLICT OF INTEREST

The authors declare that there is no conflict of interests regarding the publication of this manuscript.

REFERENCES

 Zandalinas SI, Fritschi FB, Mittler R. Global Warming, Climate Change, and Environmental Pollution: Recipe for a Multifactorial Stress Combination Disaster. Trends Plant Sci. 2021;26(6):588-599.

- Munagapati VS, Yarramuthi V, Kim D-S. Methyl orange removal from aqueous solution using goethite, chitosan beads and goethite impregnated with chitosan beads. J Mol Liq. 2017;240:329-339.
- 3. Hagan E, Castro-Soto I, Breault M, Poulin J. The lightfastness of early synthetic organic dyes. Heritage Science. 2022;10(1).
- Al-Ghouti MA, Da'ana DA. Guidelines for the use and interpretation of adsorption isotherm models: A review. J Hazard Mater. 2020;393:122383.
- Yang Z, Sun P-F, Li X, Gan B, Wang L, Song X, et al. A Critical Review on Thin-Film Nanocomposite Membranes with Interlayered Structure: Mechanisms, Recent Developments, and Environmental Applications. Environmental Science and Technology. 2020;54(24):15563-15583.
- Goga F, Dudric R, Bizo L, Avram A, MĂRincaŞ A-H, Varhely Jr C, et al. Influence of the Ni/Mg Ratio on the Colour of Spinel Pigments Prepared By A Modified Sol – Gel Method. Studia Universitatis Babeş-Bolyai Chemia. 2017:261-270.
- Preface. Nanoscience and Nanotechnology Series: Royal Society of Chemistry; 2022. p. P007-P007.
- Yergaziyeva GY, Dossumov K, Mambetova MM, Strizhak PY, Kurokawa H, Baizhomartov B. Effect of Ni, La, and Ce Oxides on a Cu/Al₂O₃ Catalyst with Low Copper Loading for Ethanol Non-oxidative Dehydrogenation. Chemical Engineering and Technology. 2021;44(10):1890-1899.
- Cui H-J, Huang H-Z, Yuan B, Fu M-L. Decolorization of RhB dye by manganese oxides: effect of crystal type and solution pH. Geochem Trans. 2015;16(1).
- Liu Y, Chen Z, Shek C-H, Wu CML, Lai JKL. Hierarchical Mesoporous MnO₂ Superstructures Synthesized by Soft-Interface Method and Their Catalytic Performances. ACS Applied Materials and Interfaces. 2014;6(12):9776-9784.
- Bao J, Yang G, Yoneyama Y, Tsubaki N. Significant Advances in C1 Catalysis: Highly Efficient Catalysts and Catalytic Reactions. ACS Catalysis. 2019;9(4):3026-3053.
- 12. Shan Y, Shan W, Shi X, Du J, Yu Y, He H. A comparative study

- of the activity and hydrothermal stability of Al-rich Cu-SSZ-39 and Cu-SSZ-13. Applied Catalysis B: Environmental. 2020;264:118511.
- 13. Ren Y, Li Y, Wu X, Wang J, Zhang G. S-scheme Sb₂WO₂/g-C₃N₄ photocatalysts with enhanced visible-light-induced photocatalytic NO oxidation performance. Chinese Journal of Catalysis. 2021;42(1):69-77.
- 14. Guo F, Huang X, Chen Z, Cao L, Cheng X, Chen L, et al. Construction of Cu₃P-ZnSnO₃-g-C₃N₄ p-n-n heterojunction with multiple built-in electric fields for effectively boosting visible-light photocatalytic degradation of broad-spectrum antibiotics. Sep Purif Technol. 2021;265:118477.
- 15. Sun Q, Wang N, Yu J. Advances in Catalytic Applications of Zeolite-Supported Metal Catalysts. Adv Mater. 2021;33(51).
- 16. Salama RS, El-Sayed E-SM, El-Bahy SM, Awad FS. Silver nanoparticles supported on UiO-66 (Zr): As an efficient and recyclable heterogeneous catalyst and efficient adsorbent for removal of indigo carmine. Colloids Surf Physicochem Eng Aspects. 2021;626:127089.
- 17. Ammar S, Abdelhedi R, Flox C, Arias C, Brillas E. Electrochemical degradation of the dye indigo carmine at boron-doped diamond anode for wastewaters remediation. Environ Chem Lett. 2006;4(4):229-233.
- 18. Aadil M, Rahman A, Zulfiqar S, Alsafari IA, Shahid M, Shakir I, et al. Facile synthesis of binary metal substituted copper oxide as a solar light driven photocatalyst and antibacterial substitute. Adv Powder Technol. 2021;32(3):940-950.
- 19. Devrim Y, Arıca ED, Albostan A. Graphene based catalyst supports for high temperature PEM fuel cell application. Int J Hydrogen Energy. 2018;43(26):11820-11829.
- 20. Pawlicka A, Tavares FC, Dörr DS, Cholant CM, Ely F, Santos MJL, et al. Dielectric behavior and FTIR studies of xanthan gum-based solid polymer electrolytes. Electrochimica Acta. 2019;305:232-239.
- 21. Ural N. The significance of scanning electron microscopy (SEM) analysis on the microstructure of improved clay: An overview. Open Geosciences. 2021;13(1):197-218.
- 22. Nie L, Li S, Chai S, Han N, Chen Y. Photothermal catalytic oxidation of toluene with enhanced efficiency over constructed $\text{CuMn}_{2}\text{O}_{4}/\text{Mn}_{2}\text{O}_{3}$ heterojunction catalyst. Appl Surf Sci. 2022;605:154567.
- 23. Sobhani A, Alinavaz S. Co-precipitation synthesis of CuMn₂O₄/CuMnO nanocomposites without capping agent and investigation of their applications for removing

- pollutants from wastewater. Biomass Conversion and Biorefinery. 2023;14(22):28901-28911.
- 24. Alzahrani KA, Ismail AA, Alahmadi N. Heterojunction of CuMn₂O₄/CeO₂ nanocomposites for promoted photocatalytic H2 evolution under visible light. Journal of the Taiwan Institute of Chemical Engineers. 2023;143:104692.
- 25. MJA, AP, NS, KJ, PFHI, JJp. Flake-like CuMn₂O₂ nanoparticles synthesized via co-precipitation method for photocatalytic activity. Physica B: Condensed Matter. 2019;572:117-124.
- 26. Arraq RR, Kadhim SH. Synthesis and Identification of Co₃O₄·Fe₃O₄/CaO Spinel Supported Catalyst. Asian J Chem. 2018;30(11):2502-2508.
- 27. Kooshki H, Sobhani-Nasab A, Eghbali-Arani M, Ahmadi F, Ameri V, Rahimi-Nasrabadi M. Eco-friendly synthesis of PbTiO₃ nanoparticles and PbTiO₃/carbon quantum dots binary nano-hybrids for enhanced photocatalytic performance under visible light. Sep Purif Technol. 2019;211:873-881.
- 28. Zhang B, Sun L. Artificial photosynthesis: opportunities and challenges of molecular catalysts. Chem Soc Rev. 2019;48(7):2216-2264.
- 29. Ikhlaq A, Zafar M, Javed F, Yasar A, Akram A, Shabbir S, et al. Catalytic ozonation for the removal of reactive black 5 (RB-5) dye using zeolites modified with CuMn₂O₄/gC₃N₄ in a synergic electro flocculation-catalytic ozonation process. Water Sci Technol. 2021;84(8):1943-1953.
- 30. Yi T, Dai C, Gao K, Hu X. Effects of synthetic parameters on structure and electrochemical performance of spinel lithium manganese oxide by citric acid-assisted sol-gel method. J Alloys Compd. 2006;425(1-2):343-347.
- 31. Acharya L, Nayak S, Pattnaik SP, Acharya R, Parida K. Resurrection of boron nitride in p-n type-II boron nitride/Bdoped-g- C_3N_4 nanocomposite during solid-state Z-scheme charge transfer path for the degradation of tetracycline hydrochloride. Journal of Colloid and Interface Science. 2020:566:211-223.
- 32. Lipp J, Banerjee R, Patwary MF, Patra N, Dong A, Girgsdies F, et al. Extension of Rietveld Refinement for Benchtop Powder XRD Analysis of Ultrasmall Supported Nanoparticles. Chem Mater. 2022;34(18):8091-8111.
- 33. Anh-Tuan V, Van-Tu V. Preparation of MgO for Removal of Dyes and Heavy Metal from Aqueous Solution: Facially Controlling the Morphology, Kinetic, Isotherms and Thermal Dynamic Investigations. Indian Journal of Science

J Nanostruct 15(4): 2260-2270, Autumn 2025

(cc) BY